International Journal of Pharmacy and Pharmaceutical Sciences

ISSN- 0975-1491 Vol 10, Issue 5, 2018

Original Article

INHIBITION OF α-AMYLASE AND α-GLUCOSIDASE BY (6RS)-22-HYDROXY-23,24,25,26,27-PENTANOR-VITAMIN-D3-6,19-SULFUR DIOXIDE-ADDUCT, MANOALIDE AND 5β-CHOLESTANE-3α,7α,12α,24,25,26-HEXOL ISOLATED FROM ACETONE EXTRACT OF *HELIANTHUS ANNUUS* L. SEEDS

VARSHA V. SONKAMBLE[1], NILESH S. WAGH[2], LAXMIKANT H. KAMBLE[1*]

[1]School of Life Sciences, Swami Ramanand Teerth Marathwada University, Nanded (Maharashtra) 431606 India, [2]Amity Institute of Biotechnology, Amity University Mumbai (Maharashtra) 410206 India
Email: lhkamble@gmail.com

Received: 15 Feb 2018 Revised and Accepted: 22 Mar 2018

ABSTRACT

Objective: This investigation includes characterization of phytochemicals from acetone extract of *Helianthus annuus* L. seeds responsible for α-amylase and α-glucosidase inhibition revealed from *in vitro* and *in silico* approaches.

Methods: Seed extract was qualitatively and quantitatively analysed for the presence of bioactive molecules. *In vitro* α-amylase and α-glucosidase inhibition assays and kinetics studies for α-glucosidase were done. Thin layer chromatography (TLC) autography of extract was done to screen potent inhibitors and characterized by high-resolution liquid chromatography-mass spectrometry (HR LC-MS). Characterized molecules were further used for *in silico* studies.

Results: Qualitative investigation reveals the presence of flavonoids, glycosides, alkaloids, terpenoids, and steroids. Quantitative analysis for total phenolic content and total flavonoid content of the extract was 0.1±0.005 mg/ml GAE and 0.025±0.003 mg/ml QE respectively. Percent inhibition of α-amylase and α-glucosidase ascertained in presence of extract was 60.42±0.6 and 83.22±0.18 at 0.01 mg while 36.24±0.81 and 37.67±0.15 at 0.005 mg of extracts for both enzymes respectively. Kinetics studies of α-glucosidase inhibition illustrated the non-competitive type of inhibition. TLC autography inhibition patterns were characterized by HR LC-MS. Characterized molecules on docking revealed (6RS)-22-hydroxy-23,24,25,26,27-pentanor-vitamin-D3-6,19-sulfurdioxide-adduct, manoalide and 5β-cholestane-3α,7α,12α,24,25,26-hexol as the best docked molecules with lowest binding energies of-12.5,-11 and-10.2 kcal/mol for α-amylase and-14.2,-11 and-11.2 kcal/mol for α-glucosidase respectively.

Conclusion: Results clearly suggested that (6RS)-22-hydroxy-23,24,25,26,27-pentanor-vitamin-D3-6,19-sulfurdioxide-adduct, manoalide and 5β-cholestane-3α,7α,12α,24,25,26-hexol could be considered as lead molecules for the discovery of potent antidiabetic agents.

Keywords: *Helianthus annuus* L., α-amylase, α-glucosidase, Kinetics study, Molecular docking

DOI: http://dx.doi.org/10.22159/ijpps.2018v10i5.25309

INTRODUCTION

Helianthus annuus L. (Sunflower) is an important oilseed crop of the world at the third position in production next to groundnut and soybean [1, 2]. The seeds are more commonly eaten as a healthy snack or included as part of a meal through the grill, pickle, hot sauce, bacon, ranch, nacho cheese, oil etc. Hence, the importance of *Helianthus annuus* L. as a source of edible oil as well as high-quality protein is continuously increasing [3].

In addition to its nutritional benefits, sunflower seeds are also reported to have pharmacological activities which may be the result of the phytochemicals they possess. Thereby researchers are developing enthusiasm for chemical composition of *Helianthus annuus* L. which indeed found the presence of proteins, calcium, carbohydrates, fats and ash content [3]. Apart from these, phytochemicals like flavonoids, tannins, alkaloids, saponins, phytosterols, steroids and fixed oils were also reported in methanolic extracts of seeds of *Helianthus annuus* L. [4]. Caffeic acid, clorogenic acid and dicaffeoylquinic acid isolated from aqueous methanol extracts of sunflower are an addition to the list [5].

Phytochemicals extracted from *Helianthus annuus* L. seeds had been reported for a broad array of biological and pharmacological activities by several researchers [6]. Nevadensin, a bioflavonoid extracted from sunflower seeds revealed a wide range of significant biological activities like hypotensive, anti-tubercular, antimicrobial, anti-inflammatory, anti-tumour and anti-cancer [7]. Aqueous extract of sunflower seed, when assessed in vivo on an ovalbumin-induced an anti-asthmatic model of mice, proposed its potential in reducing asthma [8]. Additionally, the ingestion of sunflower cotyledon extracts demonstrated the antioxidant capacity and thereby its potency to prevent cancer and other oxidative reaction related diseases [9]. The ethanolic extract of seeds was also claimed to be antihyperglycemic when administered in streptozotocin-nicotinamide-induced diabetic rats, showing a significant decrease in blood glucose level [10].

These potential health benefits invoked the need to investigate about different dietary phenolic constituents in *Helianthus annuus* L. seed extract having the capability of inhibiting α-amylase and α-glucosidase enzymes. This is because α-glucosidase and α-amylase inhibitors can retard the liberation of glucose from dietary complex carbohydrates and delay glucose absorption, resulting in reduced postprandial plasma glucose levels and suppress postprandial hyperglycaemia [11, 12]. Consequently, α-glucosidase and α-amylase inhibitors are frequently administered to diabetics in many countries.

Thus specifically, the aim of this study was to assess and characterize the phytochemical constituents in acetone extract of *Helianthus annuus* L. seeds having the potential of inhibiting α-amylase and α-glucosidase demonstrated through *in vitro* as well as *in silico* strategies.

MATERIALS AND METHODS

Chemicals

All solvents, along with the chemicals used in the qualitative and quantitative analysis of phytochemicals as well as α-amylase inhibition assay were purchased from HiMedia Pvt. Ltd. Mumbai. Acarbose, α-glucosidase and 4-nitrophenyl, α-D-glucopyranoside (*ρ*-

NPG) were purchased from Sigma-Aldrich, India. Whereas, TLC Silica gel 60 F254 plates were purchased from Merck KGaA, Germany.

Plant material

Fresh, healthy seeds of *Helianthus annuus* L. were purchased from Yogesh Pharmacy, Nanded (Maharashtra), India. The seeds were rinsed with distilled water, dehydrated in an oven at 40 °C and crushed into a fine powder using mixer grinder. 20 gm of crushed powder was then used for extraction.

Extraction

Extraction of *Helianthus annuus* L. seed was carried out by hot percolation, using Soxhlet apparatus. Sequential extraction was done using solvents of increasing polarity. The progression used was petroleum ether, ethyl acetate, chloroform, acetone, ethanol, and water individually. Extraction of each solvent was continued for 6 to 7 h and the temperature maintained was lower than the boiling points of individual solvents [13]. Depending upon our preliminary studies, acetone extract was used for further experimentation (data not shown).

Qualitative tests for phytochemical analysis

Acetone extract of *Helianthus annuus* L. was tested for presence of bioactive compounds like proteins, carbohydrates, phenols and tannins, flavonoids, saponins, glycosides, steroids, terpenoids, alkaloids, phlobatannins, fixed oils and fatty acids using standard methods of Sofowara, Trease and Harbone [14, 15].

Quantitative tests for phytochemical analysis

Total phenolic content

The amount of phenols in acetone extract was determined by Folin-Ciocalteu reagent method with a few changes. 2.5 ml of 10 % folin-ciocalteu reagent and 2 ml of 2 % solution of sodium carbonate was added to 1 ml of seed extract. The subsequent mixture was incubated for 15 min at room temperature. The absorbance of the sample was measured at 765 nm. Gallic acid was used as standard (1 mg/ml). All the tests were performed in triplicates. The outcomes were determined from the standard curve and were expressed as gallic acid equivalent (GAE) (mg/g of the extracted compound) [16].

Total flavonoid content

Aluminium chloride colourimetric method was used with a few alterations to determine flavonoid content. 1 ml of sample seed extract was mixed with 3 ml of methanol, 0.2 ml of 10 % aluminium chloride, 0.2 ml of 1 M potassium acetate and 5.6 ml of distilled water and kept at room temperature for 30 min. The absorbance was measured at 420 nm. Quercetin was used as standard (1 mg/ml). All the tests were performed in triplicates. Flavonoid contents were determined from the standard curve and were expressed as quercetin equivalent i.e. QE mg/g of extracted compound [16].

TLC autography for the screening of α-amylase inhibitors

Thin-layer chromatography was performed on the TLC silica gel 60 F254 plates. Seed extract was spotted on the plate using a micropipette and allowed to dry. One dimensional TLC analysis was performed with our optimized solvent system of acetic acid: acetone: water (6:3.5:0.5) [17]. Spots were seen under Ultra-Violet light (UV light) at 254 nm and 366 nm. When separated bands were visible on TLC plate, it was then incubated in amylase solution for 30 min for the primary reaction between the enzyme and inhibitor. After incubation, the plate was taken out of the amylase solution and incubated in 1 % starch buffer of pH 6.9 for 10-20 min for enzyme-substrate reaction and later washed with Gram's Iodine solution and observed [13].

α-amylase inhibition assay

This assay was conducted using a standard method of Dinitro-salicylic reagent [18] with a few alterations to investigate the inhibitory potential of α-amylase in presence of seed extract. In this assay, reaction mixture constituting 0.01 mg/ml and 0.005 mg/ml concentrations of seed extracts, 50 µl of phosphate buffer (0.02 M, pH 6.9) containing α-amylase solution (0.5 mg/ml) was incubated at 25 °C for 30 min. At the end of incubation, 125 µl of 1 % starch buffer (0.02 M, pH 6.9) as substrate was added to each tube at 5 s intervals. The reaction mixtures were then again incubated at 25 °C for 10 min. To terminate the reaction, 500 µl of dinitrosalicylic acid (DNSA) reagent was added and kept in boiling water bath for 5 min. Reaction tubes were allowed to cool to room temperature followed by addition of 2.5 ml distilled water to dilute the reaction mixture. The absorbance was measured at 540 nm and percent inhibition of α-amylase activity by given concentration of seed extract was calculated using the following formulae:

$$\% \text{ Inhibition} = \frac{[(\text{A540 Control} - \text{A540 Extract})] \times 100}{\text{A540 Control}}$$

α-glucosidase inhibition assay

The inhibitory potency of seed extract against α-glucosidase activity was determined in 96-well micro-titer plate by earlier reported methods with slight modifications [19]. 5 µl of 0.01 mg and 0.005 mg concentration of seed extract was incubated individually with 5 µl of (0.25 U/ml) α-glucosidase enzyme for 15 min. The mixture was then added to 25 µl of phosphate buffer containing *ρ*-NPG (5 mmol, pH 6.9) and final volume of the reaction mixture was made up to 180 µl by adding phosphate buffer (0.1 M, pH 6.9). The absorbance of the reaction was measured at 415 nm after 10 min of incubation [20]. Percent inhibition of α-glucosidase activity by given concentration of seed extract was calculated using the following formulae:

$$\% \text{ Inhibition} = \frac{[(\text{A415 Control} - \text{A415 Extract})] \times 100}{\text{A415 Control}}$$

α-glucosidase kinetic study

Seed extract was evaluated for its effect on enzyme kinetics of inhibiting α-glucosidase activity using increasing concentrations of the substrate (*ρ*-NPG, 2 mmol-10 mmol) in absence or presence of inhibitors at different concentrations. The mode of inhibition (i.e. competitive, non-competitive, or uncompetitive) of seed extract was evaluated based on inhibitory effects on Km (dissociation constant) and Vmax (maximum reaction velocity) of the enzyme. This was determined using a Lineweaver–Burk plot analysis [21].

HR LC-MS analysis

Separated bands showing positive outcomes in TLC autography were scratched out and processed for characterization of chemical constituents in them. This was done using HR LC-MS, Agilent Technologies, model: 1290 Infinity UHPLC System, 1260 infinity Nano HPLC with Chipcube, 6550 iFunnel Q-TOF.

Molecular docking

Preparation of protein structures

Protein Data Bank (PDB) 3-Dimensional (3D) structures of α-amylase (PDB Code: 3BC9) and α-glucosidase (PDB Code: 2QMJ) were obtained from PDB (http://www. rcsb. org). Using AutoDock Tools-1.5.6, [22, 23] those 3D structures were prepared as per recommended steps recommended in AutoDock tutorial [24]. These final refined structures were then used for molecular docking.

Preparation of ligand molecules

The structures of molecules identified from HR LC-MS analysis were downloaded from PubChem database (http://pubchem.ncbi.nlm.nih.gov) and ChemSpider [25] in Mol/SD format. Using Open Babel software [26], these structures were converted to PDB formats and filtered by Lipinski rule software (http://www.scfbio-iitd.res.in/software/drugdesign/lipinski.jsp) [27]. In addition to these molecules, structures of standard inhibitors like acarbose, metformin, miglitol, and voglibose were also filtered by Lipinski rule software. Molecules obeying all the five rules of Lipinski were further processed as per recommended steps in AutoDock tutorial.

Molecular docking analysis

Molecular docking or binding interaction of both α-amylase and α-glucosidase enzymes with individual ligand molecules was performed using AutoDock Vina via PyRx software to obtain several possible conformations of the ligand at the binding site of the enzyme. After completion of docking, the binding energies

(kcal/mol) of each ligand with both the individual enzymes were obtained. The best confirmation of each ligand with a respective enzyme having lowest binding energy was chosen for further study.

Interfering amino acids and their interactions involved

Obtained conformations of the enzyme-ligand complex were analysed for specific amino acids involved in ligand binding sites of respective enzymes along with the type of interactions like Vander Waals, hydrogen bonding etc involved in the docking. This was performed using the Discovery Studio 4.1 Visualizer (http://accelrys.com/products/discovery-studio) [28]. Docked structures showing amino acid residues involved in the docking as well as the interactions between respective residues and ligand were image captured using image save option in Discovery Studio 4.1 Visualizer.

3D Ligand Site analysis

For interpretation of amino acid residues involved in ligand binding site of both the enzymes, α-amylase and α-glucosidase enzymes were subjected independently to the 3DLigandSite server (http://www.sbg.bio.ic.ac.uk/3dligandsite) [29]. This server works on the basis of prediction of amino acid residues involved at binding sites through a binding site library comprising of protein-ligand complexes.

PASS analysis

Prediction of active spectra for substances (PASS) Online) is a web server (http://www.pharmaexpert.ru/passonline/) [30] which facilitates the assessment of the general biological potential of an organic drug-like molecule like specific toxicities, mechanisms of action, and pharmacological effects that might be revealed by specific molecules. Here, SD files (.sdf) or MOL file (. mol) formats of ligands were subjected to the server. The assessment values were ranged from 0.000 to 1.000 and only those molecules were considered for further evaluation whose activity is Pa>Pi (Pa= Probability to be active; Pi= Probability to be inactive) [31].

ADMET prediction

Absorption, distribution, metabolism, excretion and toxicity (ADMET) properties of drug candidates or environmental chemicals are a fundamental part in drug discovery and environmental hazard assessment. For assessment of ADMET properties molecules showing positive results in PASS analysis were submitted to server entitled admet SAR which provides ADMET structure-activity relationship (SAR) (http://lmmd.ecust.edu.cn/admetsar1/) [32]. Various properties such as blood-brain barrier, human intestinal absorption, AMES toxicity, carcinogenicity, and biodegradation for submitted molecules were calculated using this server.

RESULTS

Qualitative tests for phytochemical analysis

The phytochemical characteristics of acetone extract of *Helianthus annuus* L. seeds were tested and summarized in the table 1. Analysis revealed the presence of medically active compounds like steroids, flavonoids, glycosides, terpenoids and alkaloids in the extracts.

Table 1: Qualitative tests for phytochemical analysis

S. No.	Tests	Presence/Absence of phytoconstituents*
1	Proteins	Absent
2	Carbohydrates	Absent
3	Phenols and Tannins	Absent
4	Flavonoids	Present
5	Saponins	Absent
6	Glycosides	Present
7	Steroids	Present
8	Terpenoids	Present
9	Alkaloids	Present
10	Fixed oil and Fatty acids	Absent
11	Phlobatannins	Absent

* indicates experiment performed in triplicate

Quantitative tests for phytochemical analysis

Total phenolic and flavonoid contents

The total phenolic content of the extract was determined by Folin-Ciocalteu reagent method and measured in terms of GAE showed 0.1 mg/ml concentration whereas, the total flavonoid content measured in terms of QE showed 0.025 mg/ml concentration as depicted in the table 2.

TLC autography for the screening of α-amylase inhibitors

To screen-specific molecules acting as α-amylase inhibitors in the seed extract TLC autography was performed. Here separated bands demonstrating blue stains upon iodine staining on TLC plate were considered positive for TLC autography. Blue stained bands indicated presence of different mixtures of molecules or fractions responsible for α-amylase inhibition. This blue stain at that position was attributed to presence of starch which was not hydrolysed and thereby forming a starch-iodine complex. This was because of the inhibition of α-amylase activity by the compounds present in those fractions at that position. The TLC analysis revealed three bands in the extract when observed under UV light (at 366 nm). Blue spots were observed on two positions on the TLC plate as shown in fig. 1 i.e., at positions one and three labelled from the sample loading end. The third band was showing higher colour intensity as compared to the first. Hence the third fraction was chosen for further analysis.

Table 2: Quantitative tests for phytochemical analysis

S. No.	Tests	Concentrations*
1	Total Phenolic Content	0.1±0.005 mg/ml GAE
2	Total Flavonoid Content	0.025±0.003 mg/ml QE

*indicates mean±standard deviation values of an experiment performed in triplicate

α-amylase inhibition assay

This assay was performed to assess the inhibition of α-amylase by acetone extract of *Helianthus annuus* L. seed. Inhibition of α-amylase by the extract was calculated and presented in table 3. As compared to the control reaction, the extract showed 60.42±0.6 % inhibition at 0.01 mg and 36.24±0.81 % inhibition at 0.005 mg concentration.

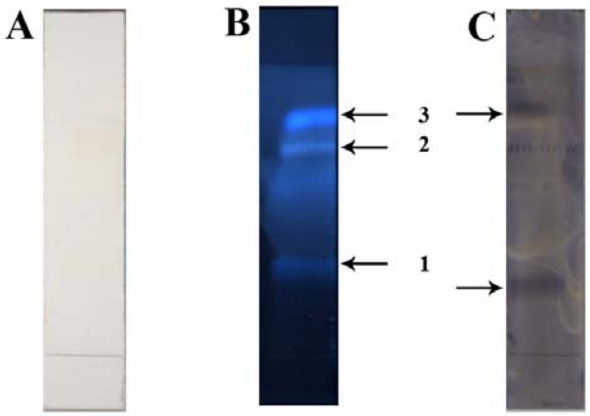

Fig. 1: TLC autography. A. TLC plate after sample run in normal light; B. TLC plate after sample run in UV light; C. TLC plate after autography treatment

Table 3: Enzyme Inhibition (percentage calculated at 0.01 and 0.005 mg concentrations)

S. No.	Enzyme	Percent inhibition at 0.01 mg	Percent inhibition at 0.005 mg
1	α-amylase	60.42±0.6	36.24±0.81
2	α-glucosidase	83.22±0.18	37.61±0.15

*indicates mean±standard deviation values of an experiment performed in triplicate

α-glucosidase inhibition assay

The activity of α-glucosidase in presence of seed extract was assessed to check the potency of extract for enzyme inhibition. Our findings reveal that 83.22±0.18 % inhibition by 0.01 mg and 37.61±0.15 % inhibition by 0.005 mg of extract was observed as represented in table 3.

α-glucosidase kinetics study

As shown in fig. 2, all the data lines on the Line weaver–Burk plots intersected in the second quadrant, demonstrating that seed extract induced a non-competitive type of inhibition. The values of Vmax and Km with respect to the concentrations of extracts are represented in table 4.

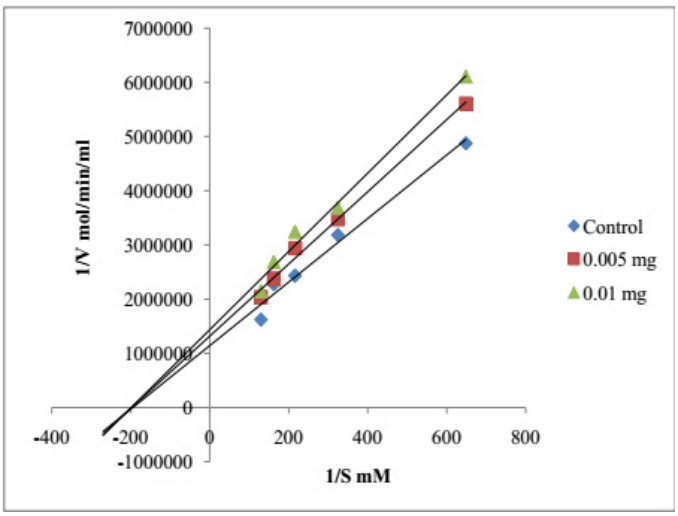

Fig. 2: Lineweaver-burk plot to determine the mode of inhibition of α-glucosidase activity by acetone extract of *Helianthus annuus* L. seeds

Table 4: α-Glucosidase inhibition kinetics analysis

S. No.	Sample	Volume used (µl)	Concentrations (mg)	*K_m (mM) x 10^{-3}	*V_{max} (mol^{-1} min^{-1} ml^{-1}) x 10^{-7}	Type of inhibition
1	Control			5.86±0.05	5±0.05	-
2	Acetone extract	2.5	0.005	6.664±0.05	5±0.05	Non-competitive inhibition
		5	0.01	7.222±0.05	5±0.05	

*indicates mean±standard deviation values of an experiment performed in triplicate

HR LC-MS analysis

The third band fraction with higher intensity and showing positive results for TLC autography was scratched out and sent for HR LC-MS analysis. As the fraction was semi-purified, around 168 molecules were obtained in the analysis. Few of them were a repetition so they were counted once while structures of only few molecules were available on the online database so as a whole 22 molecules were left with their structures available. Some of the representatives are shown in fig. 3.

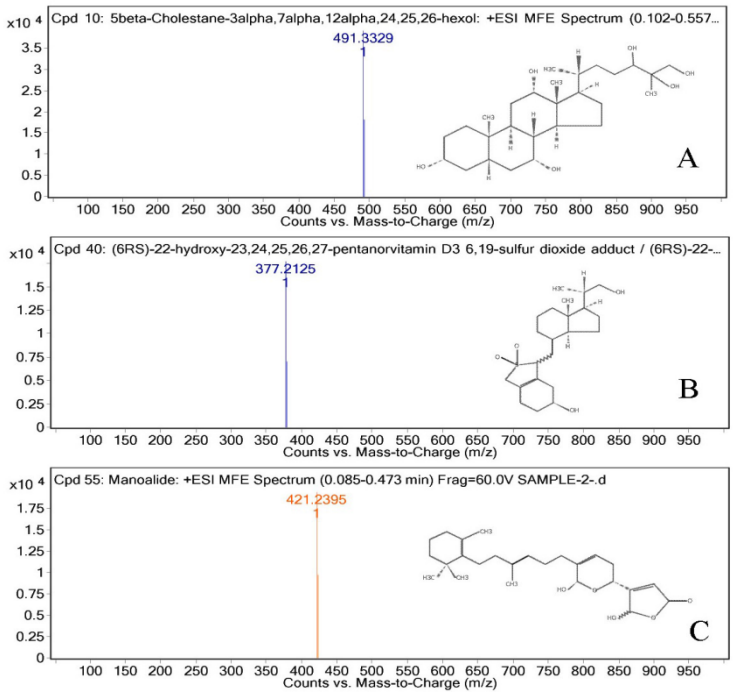

Fig. 3: Representative HR LC-MS analysis MS Spectrum of compounds. A. 5β-Cholestane-3α,7α,12α,24,25,26-hexol; B. (6RS)-22-hydroxy-23,24,25,26,27-pentanor-vitamin D3-6,19-sulfurdioxideadduct; C. Manoalide

Molecular docking analysis

All the 22 identified molecules filtered based on their potency to fulfil the Lipinski rules yielded only ten molecules as ligands for docking study. Miglitol was used as a standard inhibitor molecule for the comparison as it was alone capable of satisfying all the five rules of Lipinski in comparison to acarbose, metformin, and voglibose standards [33, 34]. The ligand molecules along with the standard miglitol were docked into the binding pockets of α-amylase and α-glucosidase to find out their binding interactions.

The docking results revealed different values of binding energies expressed in kcal/mol. All ten molecules showed lower binding energies with both the enzymes as compared to binding energies shown by miglitol (-6.1 and-5.9 kcal/mol for α-amylase and α-glucosidase respectively). When representing the best three molecules of the rest, (6RS)-22-hydroxy-23,24,25,26,27-pentanor-vitamin-D3-6,19-sulfurdioxide-adduct showed lowest binding energy followed by Manoalide and 5β-Cholestane-3α,7α,12α,24,25,26-hexol with scores of-12.5,-11 and-10.2 kcal/mol for α-amylase and-14.2,-11 and-11.2 kcal/mol for α-glucosidase respectively as depicted in table 5.

Table 5: Binding energies (kcal/mol) of compounds identified by HR LC-MS analysis and filtered by Lipinski rule with α-amylase and α-glucosidase predicted through the virtual docking

S. No.	Ligands (Molecules)	Binding energies with α-Amylase	Binding energies with α-Glucosidase
1	Miglitol*	-6.1	-5.9
2	(6RS)-22-hydroxy-23,24,25,26,27-pentanor-vitamin-D3-6,19-sulfurdioxide-adduct	-12.5	-14.2
3	Manoalide	-11	-11
4	5β-Cholestane-3α,7α,12α,24,25,26-hexol	-10.2	-11.2

*Miglitol = a standard inhibitor.

Interfering amino acids and their interactions involved

The three best molecules obtained after docking analysis were then continued for prediction of different amino acid residues involved in the interactions between these protein-ligand complexes using Discovery Studio Visualizer 4.1.

Different parameters were studied including, hydrogen bond interactions, π-π interactions, binding energy, root mean square deviation (RMSD) of active site residues and orientation of the docked compound within the active site [35]. Some of them are represented in table 6.

Whereas, 2D images of three best-docked molecules along with a standard inhibitor miglitol with both α-amylase and α-glucosidase are shown in fig. 4 and fig. 6; while 3D images are shown in fig. 5 and fig. 7 respectively.

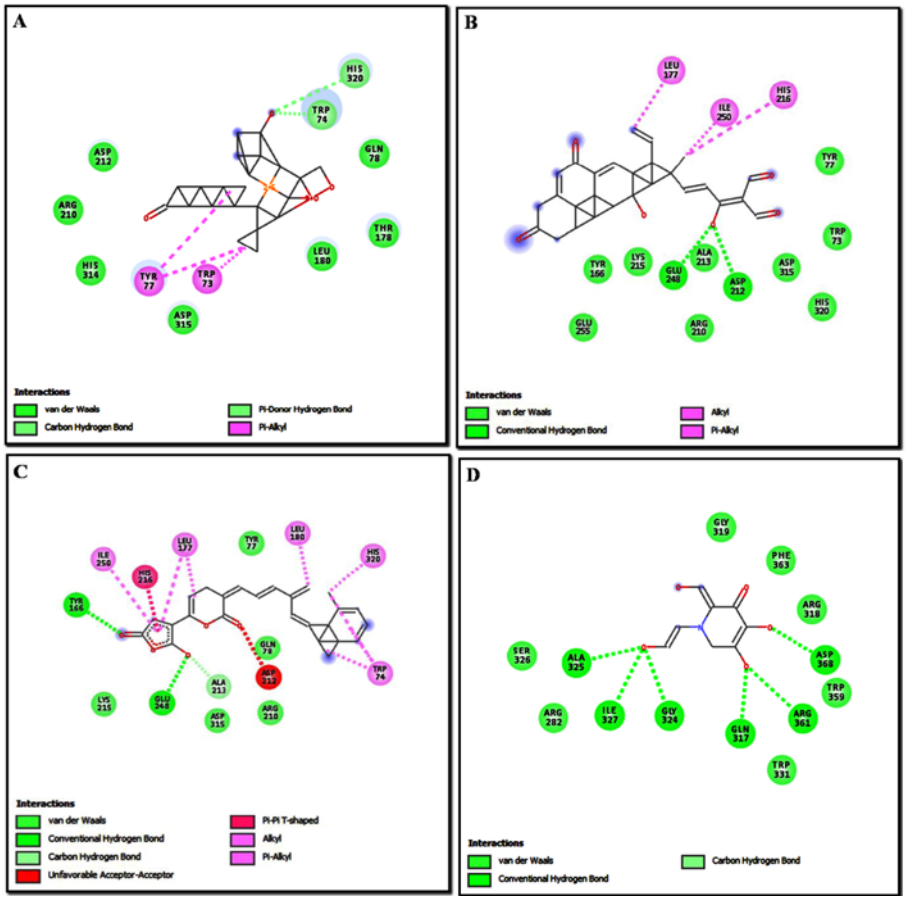

Fig. 4: 2D images generated using discovery studio 4.1 Visualizer showing amino acid residues involved in interactions between α-amylase and ligands. Here, the standard inhibitor and best three molecules with maximum binding energies are represented, where-A. (6RS)-22-hydroxy-23,24,25,26,27-pentanor-vitamin-D3-6,19-sulfurdioxide-adduct and α-amylase complex; B. 5β-Cholestane-3α,7α,12α,24,25,26-hexol and α-amylase complex; C. Manoalide and α-amylase complex; D. Miglitol and α-amylase complex

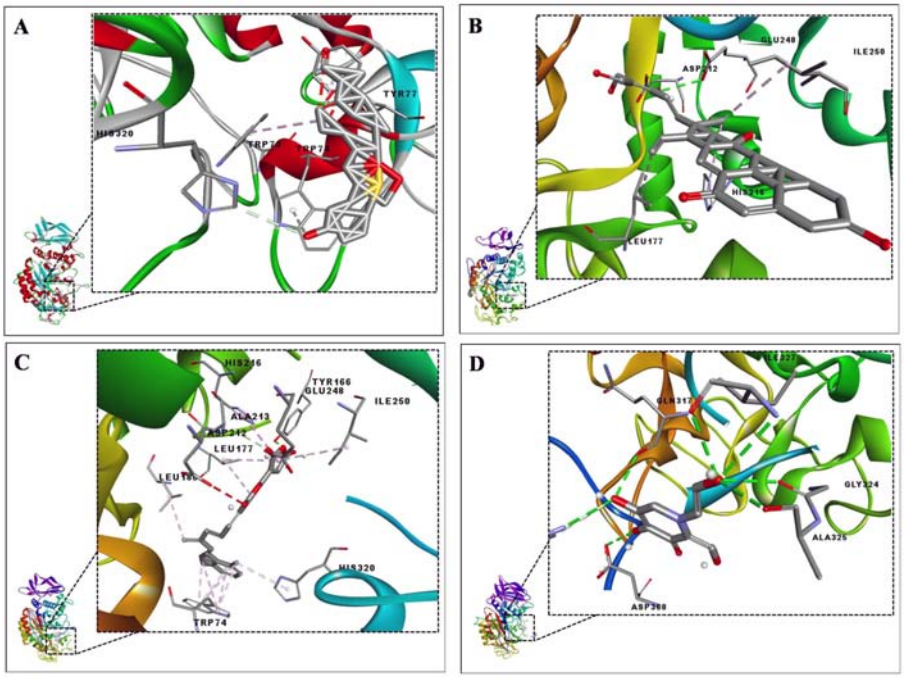

Fig. 5: 3D images generated using discovery studio 4.1 visualizer showing amino acid residues involved in interactions between α-amylase and ligands. Here, the standard inhibitor and best three molecules with maximum binding energies are represented, where-A. (6RS)-22-hydroxy-23,24,25,26,27-pentanor-vitamin-D3-6,19-sulfurdioxide-adduct and α-amylase complex; B. 5β-Cholestane-3α,7α,12α,24,25,26-hexol and α-amylase complex; C. Manoalide and α-amylase complex; D. Miglitol and α-amylase complex

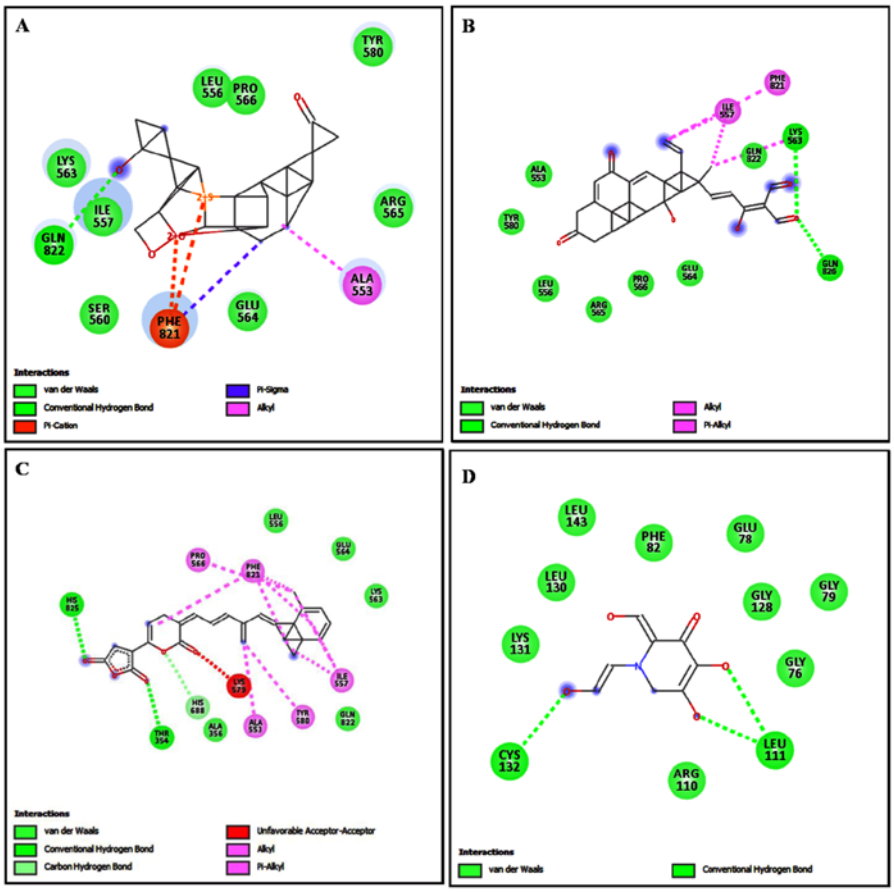

Fig. 6: 2D images generated using Discovery Studio 4.1 Visualizer showing amino acid residues involved in interactions between α-glucosidase and ligands. Here, the standard inhibitor and best three molecules with maximum binding energies are represented, where- A. (6RS)-22-hydroxy-23,24,25,26,27-pentanor-vitamin-D3-6,19-sulfurdioxide-adduct and α-glucosidase complex; B. 5β-Cholestane-3α,7α,12α,24,25,26-hexol and α-glucosidase complex; C. Manoalide and α-glucosidase complex; D. Miglitol and α-glucosidase complex

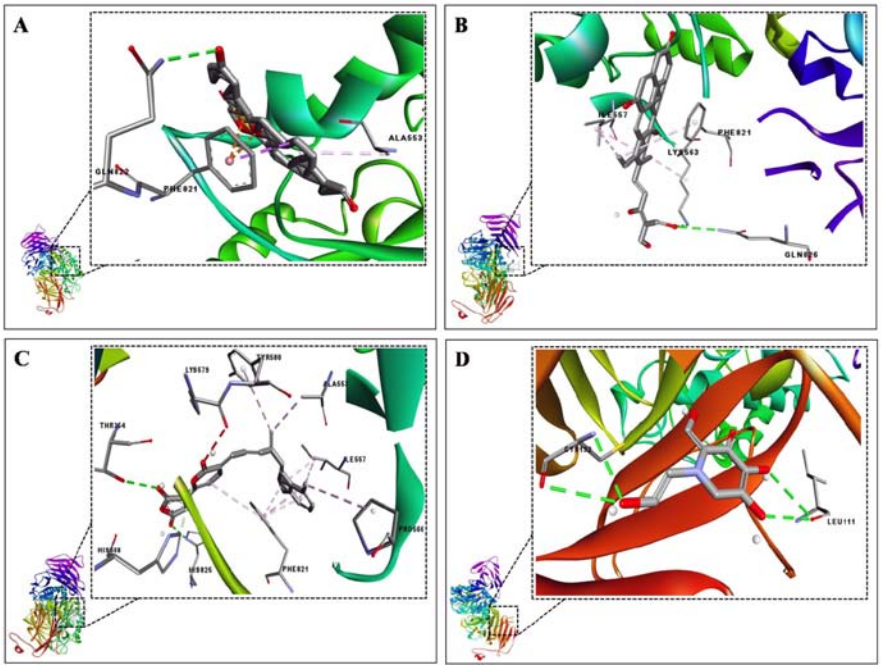

Fig. 7: 3D images generated using Discovery Studio 4.1 Visualizer showing amino acid residues involved in interactions between α-glucosidase and ligands. Here, the standard inhibitor and best three molecules with maximum binding energies are represented, where- A. (6RS)-22-hydroxy-23,24,25,26,27-pentanor-vitamin-D3-6,19-sulfurdioxide-adduct and α-glucosidase complex; B. 5β-Cholestane-3α,7α,12α,24,25,26-hexol and α-glucosidase complex; C. Manoalide and α-glucosidase complex; D. Miglitol and α-glucosidase complex

Table 6: Amino acid residues of α amylase and α-glucosidase showing different interactions in the company of ligands predicted using Discovery Studio Visualizer 4.1

S. No.	Molecules	α-Amylase amino acid residues showing different interactions			α-Glucosidase amino acid residues showing different interactions		
		Van der Waal's interactions	Conventional hydrogen Bond	Carbon hydrogen bond	Van der waal's interactions	Conventional hydrogen bond	Carbon hydrogen bond
1	Miglitol	SER 326; ARG 282; TRP 331; TRP 359; ARG 318; PHE 363; GLY 319	ALA 325; ILE 327; GLY 324; GLN 317; ARG 361; ASP 368	-	LYS 131; LEU 130; LEU 143; PHE 82; GLU 78; GLY 128; GLY 76; GLY 79; ARG 110	CYS 132; LEU 111	-
2	(6RS)-22-hydroxy-23,24,25,26,27-pentanor-vitamin-D3-6,19-sulfurdioxide-adduct	ASP 212; ARG 210; HIS 314; ASP 315; LEU 180; THR 178; GLN 78	TRP 74; HIS 320	-	LYS 563; ILE 557; SER 560; GLU 564; ARG 565; TYR 580; PRO 566; LEU 556	GLN 822	-
3	Manoalide	LYS 215; ASP 315; ARG 210; GLN 78; TYR 77	TYR 166; GLU 248	ALA 213	ALA 356; GLN 822; LYS 563; GLU 564; LEU 556	HIS 825; THR 354	HIS 688
4	5β-Cholestane-3α,7α,12α,24,25,26-hexol	GLU 255, TYR 166; LYS 215; ALA 213; ARG 210; ASP 315; HIS 320; TRP 73; TYR 77	GLU 248; ASP 212	-	ALA 553; TYR 580; LEU 556; ARG 565; PRO 566; GLU 564; GLN 822	LYS 563; GLN 826	-

3DLigand site analysis

On submission of 3D structures of both the enzymes independently to the 3DLigandSite server, a list of amino acids from respective enzymes predicted for being involved in ligand binding was obtained. Similarity was observed on comparison of these findings with that of the amino acid predictions done using Discovery studio Visualizer 4.1 software.

PASS analysis

PASS analysis was used for calculating two probabilities of molecules i.e., probability of a molecule to be active or inactive (Pa and Pi) [31, 36]. Best three molecules based on docking reports were uploaded to PASS online server in the form of SD file (. sdf) or MOL file (. mol) formats. Additionally, a standard inhibitor miglitol was also submitted for PASS prediction. PASS analysis revealed that all the three molecules and standard miglitol have potential to act as α-glucosidase inhibitors. Molecules with their Pi and Pa values are represented in table 7. Analysis also demonstrated the probability of (6RS)-22-hydroxy-23,24,25,26,27-pentanor-vitamin-D3-6,19-sulfurdioxide-adduct and miglitol of having anti-diabetic activity.

ADMET prediction

ADMET and SAR properties of the three molecules and standard miglitol showing positive results in PASS analysis were predicted using server admetSAR. The obtained analysis reports are shown in table 8 and table 9. Overall analysis revealed the potential of all the three molecules to be considered as having drug-like properties based on ADMET and SAR criteria used for prediction.

Table 7: PASS online prediction reports of molecules with Pa>Pi values along with their activities predicted at different values

S. No.	Molecules	Formula	Pa value	Pi value	Activity
1	Miglitol	$C_8H_{17}NO_5$	0.486	0.007	α-Amylase inhibitor
			0.802	0.001	α-Glucosidase inhibitor
			0.658	0.008	Antidiabetic
2	(6RS)-22-hydroxy-23,24,25,26,27-pentanor-vitamin-D3-6,19-sulfurdioxide-adduct	$C_{22}H_{34}O_4S$	0.252	0.113	Antidiabetic
			0.093	0.035	α-Glucosidase inhibitors
3	Manoalide	$C_{25}H_{36}O_5$	0.081	0.047	α-Glucosidase inhibitors
4	5β-Cholestane-3α,7α,12α,24,25,26-hexol	$C_{27}H_{48}O_6$	0.069	0.064	α-Glucosidase inhibitors

Table 8: ADMET predicted profile for active compounds

Model	Molecules			
	Miglitol	(6RS)-22-hydroxy-23,24,25,26,27-pentanor-vitamin-D3-6,19-sulfur dioxide-adduct	Manoalide	5β-Cholestane-3α,7α,12α,24,25,26-hexol
Absorption				
Blood brain barrier	-	+	+	+
Human intestinal absorption	+	+	+	+
Caco-2 permeability	-	-	-	-
P-glycoprotein substrate	S	S	S	S
P-glycoprotein inhibitor	NI	NI	NI	NI
	NI	NI	I	NI
Renal organic cation transporter	NI	NI	NI	NI
Distribution				

Metabolism				
CYP450 2C9 S	NS	NS	NS	NS
CYP450 2D6 S	NS	NS	NS	NS
CYP450 3A4 S	NS	S	S	S
CYP450 1A2 I	NI	NI	NI	NI
CYP450 2C9 I	NI	NI	NI	NI
CYP450 2D6 I	NI	NI	NI	NI
CYP450 2C19 I	NI	NI	NI	NI
CYP450 3A4 I	NI	NI	NI	NI
CYP inhibitory promiscuity	Low	Low	Low	Low
Excretion				
Toxicity				
Human ether-a-go-go-related	WI	WI	WI	WI
gene inhibition	NI	I	NI	NI
AMES toxicity	NT	NT	NT	NT
Carcinogens toxicity	NC	NC	NC	NC
Fish toxicity	Low	High	High	High
Tetrahymena pyriformis	Low	High	High	High
toxicity				
Honey bee toxicity	Low	High	High	High
Biodegradation	NB	NB	NB	NB
Acute oral toxicity	III	III	I	III
Carcinogenicity (Three-class)	No	No	No	No

+: Positive; -: Negative; S: Substrate; NS: Non-Substrate; I: Inhibitor; WI: Weak Inhibitor NI: Non-Inhibitor; NT: Non-Toxic; NC: Non-Carcinogenic; NB: Not ready biodegradable; No: Not Required.

Table 9: ADMET predicted profile regression

Model	**Molecules**			
	Miglitol	**(6RS)-22-hydroxy-23,24,25,26,27-pentanor-vitamin-D3-6,19-sulfur dioxide-adduct**	**Manoalide**	**5β-Cholestane-3α,7α,12α,24,25,26-hexol**
Absorption				
Aq. Solubility (Log S)	-0.22	-3.59	-3.75	-3.1
Caco-2 permeability (Log	-0.02	0.52	0.69	0.65
P app, cm/s)				
Distribution				
Metabolism				
Excretion				
Toxicity				
Rat (LD 50, mol/kg)	1.74	2.42	4.26	2.68
Fish (pLC50, mg/l)	2.83	1.3	0.7	1.64
Tetrahymena pyriformis	-0.52	0.59	1.06	0.79
(pIGC50, ug/l)				

DISCUSSION

Helianthus annuus L. is one of the herbs with therapeutic esteem and is utilized worldwide as nourishment and medication [3, 6]. Because of its daily consumption in human life, it can also be considered as a functional food. Its phytochemical constituents contribute in number of traditional uses for human welfare. So, this study was planned by us with a focus on analysis of phytochemicals present in the *Helianthus annuus* L. seed extracts followed by their characterization. Based on our preliminary studies using sequential extraction of sunflower seeds (data not shown), acetone extract was focused in this study. To determine the phytochemicals in acetone extract of seed, both qualitative and quantitative analysis was done. Our qualitative analysis revealed the presence of flavonoids, glycosides, steroids, terpenoids, and alkaloids. While quantitative analysis data showed that the phenolic content was 0.1 mg/ml GAE while 0.025 mg/ml QE was the total flavonoid content.

Helianthus annuus L. seed acetone extract was semi-purified and screened for the presence of α-amylase and α-glucosidase inhibitors. From this screening, it was found that concentration of 0.01 mg semi-purified seed extract could show an inhibition of 60.42±0.6 and 83.22±0.18 % of α-amylase and α-glucosidase enzyme activity respectively. Moreover, when the concentration of semi-purified *Helianthus annuus* L. seed extract was reduced to half i.e. 0.005 mg, the extract showed 36.24±0.81 and 37.61±0.15 % inhibition of α-amylase and α-glucosidase enzyme activity respectively. Enzyme inhibition kinetics in presence and absence of inhibitor was further studied only for α-glucosidase activity wherein the mode of inhibition was predicted, and it was found to be the non-competitive type of inhibition.

Different extracts of *Helianthus annuus* L. seed inhibiting α-amylase and α-glucosidase have been reported earlier but the specific molecules in those respective extracts with potency to inhibit α-amylase and α-glucosidase were not yet reported [6, 10]. In the present study, using our devised methodology of TLC autography, we could screen crude acetone extract of *Helianthus annuus* L. showing inhibitory activity, followed by semi-purification of fraction scratched from TLC plate and finally characterization of bioactive phytochemicals in the semi-purified fraction by HR LC-MS.

HR LC-MS analysis uncovered the presence of various molecules which were hypothesized to have enzyme inhibition potential. Literature survey confirmed our hypothesis that few of molecules characterized in our extracts like madecassic acid, linoleamide, cephaeline, and phenylethylamine were reported for antidiabetic properties [37-40]. However, when these molecules were filtered for Lipinski rule, all of them could not pass the rule and hence were not a suitable lead. So, it was necessary to filter 168 HR LC-MS characterized molecules via Lipinski rule which thereby yielded ten molecules fulfilling the criteria.

These ten molecules along with a standard inhibitor miglitol were successfully docked *in silico* with both α-amylase and α-glucosidase enzymes to find the enzyme-ligand interactions. Out of ten, (6RS)-22-hydroxy-23,24,25,26,27-pentanor-vitamin-D3-6,19-sulfur

dioxide-adduct, Manoalide and 5β-Cholestane-3α,7α,12α,24,25,26-hexol demonstrated lowest binding energies therefore could be considered as potential inhibitors for α-amylase as well as α-glucosidase. Further, comparing the investigation performed using Discovery Studio 4.1 Visualizer and 3DLigandSite server; we found that similar amino acid residues were involved in the ligand binding site of both enzymes. Use of *in silico* molecular docking thus proves to be an effective way for screening a large number of lead molecules interacting with the enzyme as a target thereby reducing time and expenses for *in vivo* studies.

Further, three best molecules from molecular docking analysis were assessed for PASS analysis to predict their active spectra. This analysis revealed that all three molecules have the potential of α-glucosidase inhibitory activity. Thus, these three molecules were then considered as lead and tested for ADMET and SAR prediction.

It is well known that ADMET properties of chemicals or drug candidates play an important role in drug discovery as well as an environmental hazard assessment [41, 42]. Using admetSAR server, absorption predictions of the molecules for various models like a blood-brain barrier (BBB), human intestinal absorption (HIA), Caco-2 permeability, P-glycoprotein substrate, P-glycoprotein inhibitors, and renal organic cation transporter were checked. In case of metabolism, predictions for drug metabolism by cytochrome P450 (CYP) group of isozymes were checked; and in case of toxicity prediction, all the toxicity models like fish toxicity, AMES toxicity, *Tetrahymena pyriformis* toxicity, honey bee toxicity, biodegradation, acute oral toxicity, carcinogens toxicity, etc were checked. Obtained regression values revealed that a portion of the models was predicted with potent risks and thereby indicated unfavourable results. However, they have very low predicted probability values and in comparison, with probability values obtained from standard drug miglitol all the three molecules from our study could show drug-like properties or strongly support the capability of molecules to act as a drug [43, 44]. So, our studies put forward this as the first report on isolation and characterization of acetone extract of *Helianthus annuus* L. seed having α-amylase and α-glucosidase inhibitory or antidiabetic potential.

CONCLUSION

Helianthus annuus L. is the hub of medicinal values and easily accessible for human utilization. So, our focus was to estimate the phytochemicals present in the acetone extract of *Helianthus annuus* L. seeds and to screen for α-amylase and α-glucosidase inhibitors *in vitro* as well as *in silico*. Considering the side effects of synthetic inhibitors available in the market, and to support a more beneficial way of life for individuals, this study was designed. Screening of phytoconstituents as α-amylase and α-glucosidase inhibitors with low or no side effects was the primary aim of this investigation. Also, here the outcome of the investigation revealed potency of seed extract towards inhibition of α-amylase as well as α-glucosidase with minimum 0.005 mg concentration. Our *in silico* study reveals that ten molecules inhibit both α-amylase and α-glucosidase better than the standard miglitol and also follow the Lipinski rule. Furthermore, the best three were (6RS)-22-hydroxy-23,24,25,26,27-pentanor-vitamin-D3-6,19-sulfur dioxide-adduct (-12.5 and-14.2 kcal/mol), Manoalide (-11 and-11 kcal/mol) and 5β-Cholestane-3α,7α,12α,24,25,26-hexol (-10.2 and-11.2 kcal/mol) respectively. Moreover, based on their PASS analysis and ADMET predictions these three molecules could be considered as lead molecules for antidiabetic drugs. However, the further detail *in vivo* investigation must be carried out before these molecules could be used as potent antidiabetic agents. (We have claimed these results for a patent with Indian Patent Authority, Ref. No./Application No.-201621036607).

ACKNOWLEDGEMENT

The authors would like to acknowledge sophisticated analytical instrument facility (SAIF), IIT-Bombay, for HR-LCMS analysis.

AUTHORS CONTRIBUTIONS

Varsha V Sonkamble designed and performed the experiments, analyzed the results and wrote the research manuscript. Nilesh S Wagh helped in the design of experiments, analyzed statistical data and coordinated in preparing the manuscript. Laxmikant H Kamble guided and corrected the manuscript.

CONFLICTS OF INTERESTS

The author(s) declare(s) that there is no conflict of interest.

REFERENCES

1. Ingale S, Shrivastava S. Chemical studies of new varieties of sunflower (*Helianthus annuus*) LSF-11 and LSF-8 seeds. Agric Biol J North Am 2011;2:1071–81.
2. Byrareddy K, Uppar DS, Vyakaranahal BS, Hiremath SM, Hunje R. Nadaf HL. Effect of integrated nutrient management on sunflower hybrid (KBSH-I) seed production. Karnataka J Agric Sci 2008;21:171-5.
3. Anjum FM, Nadeem M, Khan MI, Hussain S. Nutritional and therapeutic potential of sunflower seeds: a review. Br Food J 2012;114:544–52.
4. Rajakannu S, Sritharan UR. Phytochemical screening, antimicrobial activity and *in vitro* antioxidant investigation of methanolic extract of seeds from *Helianthus annuus* L. Chem Sci Rev Lett 2012;1:30–4.
5. Mikolajczak KL, Cecil Randolph, Smith J, Wolff IA. Phenolic and sugar components of Armavireo variety sunflower (*Helianthus annuus*) seed meal. J Agric Food Chem 1970;18:27–32.
6. Dwivedi A, Sharma G. A review on heliotropism plant: *Helianthus annuus* L. J Phytopharm 2014;3:149–55.
7. Brahmachari G. Nevadensin: isolation, chemistry and bioactivity. Int J Green Pharm 2010;4:213-9.
8. Heo JC, Woo SU, Kweon MA, Park JY, Lee HK, Son M, *et al.* Aqueous extract of the *Helianthus annuus* seed alleviate asthmatic symptoms *in vivo*. Int J Mol Med 2008;21:57–61.
9. Giada MDLR, Mancini Filho J. Antioxidant capacity of the striped sunflower (*Helianthus annuus* L.) seed extracts evaluated by three *in vitro* methods. Int J Food Sci Nutr 2009;60:395–401.
10. Saini S, Sharma S. Antidiabetic effect of *Helianthus Annuus* L., seeds ethanolic extract in streptozotocin-nicotinamide induced type 2 diabetes mellitus. Int J Pharm Pharm Sci 2013;5:382–7.
11. D'Archivio M, Filesi C, Di Benedetto R, Gargiulo R, Giovannini C, Masella R. Polyphenols, dietary sources and bioavailability. Ann Ist Super Sanita 2007;43:348–61.
12. Koleckar V, Kubikova K, Rehakova Z, Kuca K, Jun D, Opletal LJ, *et al.* Condensed and hydrolysable tannins as antioxidants influencing the health. Mini-Rev Med Chem 2008;8:436–47.
13. Sonkamble VV, Zore GB, Kamble LH. A simple method to screen amylase inhibitors using thin layer chromatography. Sci Res Report 2014;4:85–8.
14. Yadav RNS, Agarwala M. Phytochemical analysis of some medicinal plants. J Phytol 2011;3:10–4.
15. Kavit M, Patel BN, Jain BK. Phytochemical analysis of leaf extract of *Phyllanthus fraternus*. Res J Recent Sci 2013;2:12–5.
16. Aiyegoro OA, Okoh AI. Preliminary phytochemical screening and In vitro antioxidant activities of the aqueous extract of Helichrysum longifolium DC. BMC Complement Altern Med 2010;10:21.
17. Sonkamble VV, Kamble LH. Antidiabetic potential and identification of phytochemicals from *Tinospora cordifolia*. Am J Phytomed Clin Ther 2015;3:97-110.
18. Miller G. Use of dinitrosalicylic acid reagent for determination of reducing sugar. Anal Chem 1959;31:426–8.
19. Zhang J, Zhao S, Yin P, Yan L, Han J, Shi L, *et al.* the a-Glucosidase inhibitory activity of polyphenols from the burs of *castanea mollissima* blume. Molecules 2014;19:8373–86.
20. Kulsoom J, Syed SM, Saima R, Syed TM, Syed N, Itrat F, *et al.* 2-arylquinazolin-4(3H)-ones: a new class of a-glucosidase inhibitors. Bioorg Med Chem 2015;4:3–7.
21. Hati S, Madurkar SM, Bathula C, Thulluri C, Agarwal R, Amber F, *et al.* Design, synthesis and biological evaluation of small molecules as potent glucosidase inhibitors. Eur J Med Chem 2015;100:188–96.
22. Trott O, Olson AJ. AutoDock Vina: improving the speed and accuracy of docking with a new scoring function, efficient optimization, and multithreading. J Comput Chem 2009;31:455–61.
23. Morris GM, Green LG, Radic Z, Taylor P, Olson AJ, Grynszpan F. Automated docking with protein flexibility in the design of femtomolar "Click Chemistry" inhibitors of acetyl-cholinesterase. J Chem Inf Model 2014;53:898–906.

24. Dallakyan S, Olson A. Small-molecule library screening by docking with PyRx. Chem Biol 2015;19:243–50.
25. Pence HE, Williams AJ. ChemSpider: an online chemical information resource. J Chem Edu 2010;87:1123-4.
26. O'Boyle NM, Banck M, James CA, Morley C, Vandermeersch T, Hutchison GR. Open babel: an open chemical toolbox. J Cheminform 2011;3:33.
27. Lipinski C. Lead profiling Lead-and drug-like compounds: the rule-of-five revolution. Drug Discovery Today Technol 2004;1:337–41.
28. Mamgain S, Sharma P, Pathak RK, Baunthiyal M. Computer-aided screening of natural compounds targeting the E6 protein of HPV using molecular docking. Bioinformation 2015;11:236-42.
29. Wass MN, Kelley LA, Sternberg MJE. 3DLigand site: predicting ligand-binding sites using similar structures. Nucleic Acids Res 2010;38:W469–W73.
30. Poroikov VV, Filimonov DA, Ihlenfeldt W, Gloriozova TA, Lagunin AA, Borodina YV, *et al.* PASS biological activity spectrum predictions in the enhanced open NCI database browser. J Chem Inf Comput Sci 2003;43:228–36.
31. Paramashivam S, Elayaperumal K, Natarajan B, Ramamoorthy M, Balasubramanian S, Narayanan K. *In silico* pharmacokinetic and molecular docking studies of small molecules derived from *Indigofera aspalathoides* vahl targeting receptor tyrosine kinases. Bioinformation 2015;11:73–84.
32. Cheng F, Li W, Zhou Y, Shen J, Wu Z, Liu G, *et al.* admetSAR: a comprehensive source and free tool for assessment of chemical ADMET properties. J Chem Inf Model 2012;52:3099–105.
33. Kingma PJ, Menheere PPCA, Sels JP, Kruseman ACN. a-glucosidase inhibition by miglitol in NIPPM patients. Diabetes Care 1992;15:478–83.
34. Campbell LK, Baker DE, Campbell RK. Miglitol: assessment of its role in the treatment of patients with diabetes mellitus. Ann Pharmacother 2000;34:1291–301.
35. Madeswaran A, Asokkumar K, Umamaheswari M, Sivashanmugam T, Subhadradevi V, Jagannath P. *In silico* docking evaluation of α-Amylase inhibitory activity of Butein and Tricetin. J Comput Methods Mol Des 2014;4:51–6.
36. Dirar A, Waddad A, Mohamed M, Mohamed M, Wadah O, Mohammed M, *et al. In silico* pharmacokinetics and molecular docking of three leads isolated from *Tarconanthus camphoratus* L. Int J Pharm Pharm Sci 2016;8:71–7.
37. Hsu Y, Hung Y, Hu L, Lee Y, Yin M. Anti-diabetic effects of made classic acid and rotundic acid. Nutrients 2015;7:10065–75.
38. Matsubara K, Matsuzawa Y, Jiao S, Kihara S, Takama T, Nakamura T, *et al.* Cholesterol-lowering effect of N-(a-methylbenzyl) linoleamide (melinamide) in cholesterol-fed diabetic rats. Atherosclerosis 1988;72:199–204.
39. Tanwer BS, Vijayvergia R. Biological evaluation of *Alangium salviifolium* (L. F.) wangerin. J Chem Pharm Res 2014;6:611–8.
40. Abdel-aziz SA, Hussein MA, Abdel Raheem IT. Design, synthesis and antidiabetic activity of some new 4-amino (or 6-oxo)-2-methyl/benzylthio (or substituted amino) pyrimidine derivatives. Bull Pharm Sci Assiut Univ 2011;34:149–58.
41. Somani Z, Bhattacharjee R, Chodankar MNA. *In vitro* antioxidant, anti-inflammatory, inovo antiangiogenic activities and virtual screening of phytoconstituents of *Chromolena odorata*. Int J Curr Res 2014;6:7766–71.
42. Rohini K, Srikumar P. *In silico* approach of anticancer activity of phytochemical coumarins against cancer target JNKS. Int J Pharm Pharm Sci 2013;5:741–2.
43. Dhanalakshmi R, Manavalan R. *In silico* docking approach for the antiatherosclerotic activity of phytoconstituents of *Corchorus aestuans* and ADMET prediction. Asian J Pharm Clin Res 2015;8:350–3.
44. Chaluveelaveedu N, Kumar A, Nair P, Gupta N, Silakari C, Tripathi T, *et al.* Molecular docking and *in silico* ADMET study reveals Acylguanidine 7a as a potential inhibitor of β-secretase. Adv Bioinformatics 2016:1–6. http://dx.doi.org/10.1155/2016/9258578.